Multiecho Dixon Fat and Water Separation Method for Detecting Fibrofatty Infiltration in the Myocardium

Peter Kellman,[1]* Diego Hernando,[2] Saurabh Shah,[3] Sven Zuehlsdorff,[3] Renate Jerecic,[3] Christine Mancini,[1] Zhi-Pei Liang,[2] and Andrew E. Arai[1]

Conventional approaches for fat and water discrimination based on chemical-shift fat suppression have reduced ability to characterize fatty infiltration due to poor contrast of microscopic fat. The multiecho Dixon approach to water and fat separation has advantages over chemical-shift fat suppression: 1) water and fat images can be acquired in a single breathhold, avoiding misregistration; 2) fat has positive contrast; 3) the method is compatible with precontrast and late-enhancement imaging, 4) less susceptible to partial-volume effects, and 5) robust in the presence of background field variation; and 6) for the bandwidth implemented, chemical-shift artifact is decreased. The proposed technique was applied successfully in all 28 patients studied. This included 10 studies with indication of coronary artery disease (CAD), of which four cases with chronic myocardial infarction (MI) exhibited fatty infiltration; 13 studies to rule out arrhythmogenic right ventricular cardiomyopathy (ARVC), of which there were three cases with fibrofatty infiltration and two confirmed with ARVC; and five cases of cardiac masses (two lipomas). The precontrast contrast-to-noise ratio (CNR) of intramyocardial fat was greatly improved, by 240% relative to conventional fat suppression. For the parameters implemented, the signal-to-noise ratio (SNR) was decreased by 30% relative to conventional late enhancement. The multiecho Dixon method for fat and water separation provides a sensitive means of detecting intramyocardial fat with positive signal contrast. Magn Reson Med 61:215–221, 2009. © 2008 Wiley-Liss, Inc.

Key words: MRI; heart; fat; chronic myocardial infarction; arrhythmogenic right ventricular dysplasia; ARVD; arrhythmogenic right ventricular cardiomyopathy; ARVC; lipoma; phase-sensitive inversion recovery; PSIR

The ability of MRI to discriminate between water and fat is important in tissue characterization. It has been shown that fibrofatty infiltration of the myocardium is associated with sudden death (1), and therefore noninvasive detection could have high prognostic value. Conventional approaches to fat and water discrimination based on fat

[1]Laboratory of Cardiac Energetics, National Heart, Lung and Blood Institute (NHLBI), National Institutes of Health (NIH), U.S. Department of Health and Human Services (DHHS), Bethesda, Maryland, USA.

[2]University of Illinois–Urbana-Champaign, Department of Electrical and Computer Engineering, Urbana, Illinois, USA.

[3]Siemens Medical Solutions, MR Research and Development, Chicago, Illinois, USA.

*Correspondence to: Peter Kellman, Laboratory of Cardiac Energetics, National Heart, Lung and Blood Institute, National Institutes of Health, Room B1D416, Building 10, MSC-1061, 10 Center Drive, Bethesda, MD 20892-1061. E-mail: kellman@nih.gov

suppression are commonly used to characterize masses, but have a reduced ability to characterize myocardial fatty infiltration due to the poor contrast of microscopic fat and partial-volume effects. Multiecho Dixon methods (2–10) for fat and water separation provide a sensitive means of detecting small concentrations of fat with improved contrast. In this study, these methods were applied to the detection of fibrofatty infiltration observed in chronic myocardial infarction (MI) as well as cases of suspected arrhythmogenic right ventricular cardiomyopathy (ARVC). Fat and water separation was implemented both precontrast as well as applied to late enhancement using a multiecho, phase-sensitive inversion-recovery gradient-echo (PSIR-GRE) sequence.

Approaches to characterizing tissue fat content (9,10) include: 1) the use of chemical-shift saturation to suppress fat; 2) T_1-weighted imaging to detect T_1 shortening of fat, which may be observed as bright signal intensity; and 3) multiecho Dixon methods to reconstruct water- and fat-separated images (2–10). In fat-suppression imaging, regions with fat will appear dark, and the absence of signal relative to non-fat-suppressed images will indicate the presence of fat. A disadvantage of this approach is that it requires acquiring both fat-suppressed and nonsuppressed images. Furthermore, the performance of fat suppression depends on the field homogeneity. Importantly, for application in characterizing fatty infiltration in which voxels may have a low concentration of fat, the decrease in signal intensity (or negative contrast) is often difficult to discern from other signal intensity fluctuations. For this reason, the diagnosis of intramyocardial fat using conventional fat suppression can be subjective.

T_1-weighted imaging may be used to detect fat (9,10), and T_1-weighted inversion recovery (IR) has been used to detect fatty infiltration in chronic myocardial infarction (MI) (11) prior to contrast administration. In this approach, an IR-cine steady-state free precession (SSFP) sequence is used to acquire images at multiple inversion times (TIs). Regions with significant fat content have been observed to have a shorter null time. Since this technique is performed prior to contrast, it may be difficult to precisely correlate with late-enhancement images acquired at different cardiac phase and separate breath-holds. Further, additional precontrast breath-hold images must be acquired prior to obtaining the late-enhancement images, which in some cases may be the first recognition of MI.

Multiecho methods for fat and water separation are based on the difference in resonance frequencies between water and fat. Dixon's original method for water and fat separation (2) acquires two images with different echo times (TEs) chosen such that the water and fat are in-phase and opposed-phase, respectively, and may be combined to

obtain separate water and fat images. This simple method assumes that the water is exactly on resonance, which limits the performance of water and fat separation in the presence of B_0-field inhomogeneity. A three-point method (3) was introduced to allow estimation of the background field at each voxel. In this method, the TEs are also set such that the water and fat are in-phase and opposed-phase in order to simplify estimation of the background fieldmap. However, phase ambiguities arising from large field variation can still lead to incorrect assignment of water and fat pixels. Phase unwrapping (4) has been proposed to deal with this issue; however, phase unwrapping methods are often not robust in cardiac imaging applications due to high field inhomogeneity (12) as well as a relatively low signal-to-noise ratio (SNR).

Recent methods (5–8) for multiecho Dixon water and fat separation jointly estimate the fieldmap, water, and fat images. These methods apply spatial constraints in the process of fieldmap estimation, which is generally more robust than phase unwrapping. These methods may also be used with arbitrary TEs which allows for more flexible sequence and protocol design. One method to solve this nonlinear estimation problem, termed iterative decomposition with echo asymmetry and least-squares (IDEAL) (5,6), consists of repeated linearizations of the original nonlinear problem, alternatively estimating the water and fat signals and the field map. A second method is the variable projection (VARPRO) method (8), which formulates the solution as a separable nonlinear least-squares problem. VARPRO attains the globally optimum maximum-likelihood (ML) solution, and the implementation is very robust for the proposed cardiac application with large background field variation and low SNR. VARPRO was found to be more robust (8) in terms of correct classification of water and fat than our implementation of IDEAL, and therefore was used instead throughout the study.

The proposed use of multiecho Dixon water-fat separation to chacterize intramyocardial fat has a number of potential benefits. The multiecho Dixon method combined with fieldmap estimation (5–8) produces excellent discrimination between water and fat. The fat-separated image provides positive contrast (containing only signal from lipids), which improves diagnostic confidence. The proposed water- and fat-separation method may be combined with late enhancement to provide a positive correlation between fibrosis and fat, which both appear bright postcontrast. The water and fat images are spatially registered since they are reconstructed from the same multiecho dataset. Furthermore, chemical-shift artifacts may be eliminated in reconstruction.

It was hypothesized that the multiecho Dixon method of fat-water imaging could be used to detect intramyocardial fat. Multiecho GRE fat-water imaging was performed on 28 patients with either known or suspected coronary artery disease (CAD), or with suspicion of intramyocardial fat.

MATERIALS AND METHODS

Imaging

A multiecho GRE sequence was implemented with fat and water separation using the VARPRO multipoint Dixon reconstruction method (8). The imaging sequence was ECG-triggered, with two R-R intervals between inversions, and used an echo-train readout with four echoes with flyback gradients for monopolar readout. The echo-train readout was used to increase the acquisition efficiency and thereby maintain acceptable breath-hold duration. Typical parameters for imaging with the MAGNETOM Espree (Siemens AG Medical Solutions, Erlangen, Germany) 1.5T short, wide-bore scanner (33 mT/m, slew rate (SR) = 100 T/m/s, 70-cm bore diameter, 1.25-m magnet length) were: bandwidth = 977 Hz/pixel;, TE = 1.64, 4.17, 6.7, and 9.23 ms; TR = 11.2 ms; flip angle = 20−25°; image matrix = 256 × 126; views per segment = 19; and breath-hold duration = 16 heartbeats, including two initial heartbeats discarded for transition to steady state. Phase-encoded (PE) oversampling was used in cases where the matrix size was rounded up due to segmentation.

The multiecho GRE sequence incorporated an optional IR preparation for late-enhancement imaging following contrast administration. Late-enhancement imaging used phase-sensitive reconstruction (13) for TI insensitivity and to eliminate artifacts arising from magnitude detection. The IR preparation is not used precontrast. The PSIR multiecho GRE sequence acquires a proton density (PD) reference on alternate heartbeats, which was used to jointly estimate a fieldmap and fat- and water-separation matrix that was applied to the inversion-recovery (IR) images. Sensitivity maps estimated from the complex PD images were used for B_1-weighted combining with optimal noise weighting of multicoil IR and PD fat and water images (13). The PD images were also used for estimating the background phase for phase-sensitive reconstruction and for correcting surface coil intensity variation as previously described (13). The PSIR late-enhancement sequence is essentially the same as the conventional PSIR late-enhancement sequence (13) with modification for multiecho readout.

The fat is shifted slightly in the readout direction relative to the water due to the difference in resonance frequencies (9,10). With the bandwidth used in this study, the chemical shift is approximately 215 Hz/977 Hz/pixel = 0.22 pixels. The subpixel shift is generally negligible at such large bandwidths but is easily corrected in the reconstruction. One approach (14) to correct for chemical shift in multiecho fat-water separation is to correct for chemical shift by performing the fat-water separation in *k*-space after the background phase of each echo image due to field inhomogeneity has been removed.

Images were reconstructed offline using MATLAB®. The VARPRO method (8) was used to robustly estimate the field map in the presence of field inhomogeneity.

SNR Measurements

The SNRs for various protocols were measured and compared. Comparisons were made between: 1) multiecho Dixon water- and fat-separated late-enhancement images and the conventional single-echo late-enhancement approach; 2) multiecho Dixon water- and fat-separated images acquired pre- and postcontrast enhancement; and 3) multiecho Dixon water- and fat-separated images acquired precontrast and conventional turbo spin echo (TSE) im-

ages with and without chemical-shift fat suppression. SNR measurements were made both in phantoms and in vivo. SNR-scaled images (15) were reconstructed based on noise estimates derived from prescan noise acquisition.

The SNR of the water- and fat-separated late-enhancement images will be reduced relative to the conventional single-echo late-enhancement approach due to the increase in signal bandwidth. The SNR loss due to the increased bandwidth is offset to some extent by the effective signal averaging gain from combining of multiple echo images in the process of separating water and fat images. The effective number of signal averages (NSA) for the parameters used was calculated from the Cramer-Rao lower bound (CRLB) as a function of the ratio of water to fat within a voxel (16). The VARPRO method has been shown to meet the CRLB over a wide range of parameters (8). The CRLB was computed for four echoes using the TE values of the protocol used in this study.

The precontrast protocol has a higher SNR for the fat signal than the late-enhancement protocol due to the incomplete T_1 recovery following IR preparation. The water signal is approximately nulled for the late-enhancement images. An SNR comparison was made between precontrast and late enhancement using the measurement of the fat signal from epicardial fat in multiecho Dixon fat-separated images. An SNR comparison was also made using measurements of oil-phantom images using TI = 300 ms, which is typical for late enhancement. The SNR was measured and compared for both conventional single-echo turbo-FLASH and multiecho Dixon water- and fat-separated approaches using an oil phantom. The turbo-FLASH sequence used the same readout flip angle and matrix size, and had a bandwidth of 140 Hz/pixel (TE/TR = 3.2/7.6 ms).

SNR comparisons of multiecho Dixon water- and fat-separated images with conventional TSE were made using oil and water phantoms. An in vivo comparison of precontrast SNR of the fat-separated images was made with the contrast-to-noise ratio (CNR) of the fat region for precontrast TSE with and without chemical-shift fat suppression. For the CNR measurement, which is limited by the local signal inhomogeneity (see Discussion), the CNR was estimated as the signal difference between fat intensity with and without fat suppression divided by the standard deviation of a small region adjacent to the fat region in the fat-suppressed image. The TSE protocol used a bandwidth of 780 Hz/pixel, echo-train length = 21, and 180° readout flip angle. Parallel imaging with an acceleration rate of 2 was used for in vivo imaging with TSE; however, to simplify the SNR measurements, parallel imaging was not used for the phantom measurements. Therefore, the phantom measurements will have $\sim\sqrt{2}$ higher relative SNR compared to in vivo measurements.

Patient Studies

Imaging using multiecho Dixon water and fat separation was performed on 28 patients with either known or suspected CAD or suspicion of cardiac tumors or masses, or to rule out ARVC under clinical research protocols approved by the institutional review boards of the National Heart, Lung, and Blood Institute and Suburban Hospital, with
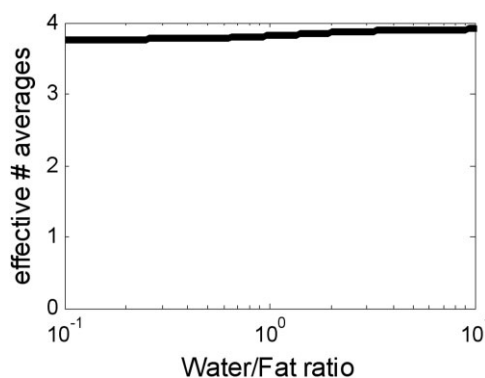

FIG. 1. Effective NSA for water and fat separation using the four-echo protocol employed in the study.

written informed consent. In patient studies with known or suspected CAD ($N = 10$), late enhancement using the conventional single-echo turbo-FLASH sequence was performed, and multiecho Dixon water- and fat-separated images were acquired postcontrast for all cases that exhibited MI. In several cases with known prior MI, multiecho Dixon water- and fat-separated images were acquired precontrast ($N = 5$) as well as postcontrast. Although fatty infiltration was not expected in cases of acute MI, water- and fat-separated imaging was performed to serve as a negative control. In studies with suspicion of cardiac masses ($N = 5$), precontrast dark-blood-prepared TSE imaging was performed with and without chemical-shift fat saturation to assess tissue characteristics. In these cases, multiecho Dixon water- and fat-separated images were acquired precontrast for all cases. In studies to rule out ARVC ($N = 13$), the standard protocol used precontrast dark-blood-prepared TSE imaging with and without chemical-shift fat saturation to assess fatty infiltration, and late enhancement to assess fibrosis. In these cases, multiecho Dixon water- and fat-separated images were acquired precontrast for all cases.

Gadolinium late-enhancement imaging was typically performed 10–20 min post contrast-agent administration (0.15 mmol/kg dose).

RESULTS

Phantom Measurement and SNR Calculation

The effective NSA for the specific four-echo protocol that was used was calculated using the CRLB to be >3.8 over a wide range of water/fat ratios (Fig. 1). The measured SNR loss of the water- and fat-separated late-enhancement (phantom) image was approximately 30% relative to the single-echo conventional late-enhancement sequence, in close agreement with the predicted loss for these specific protocols (see Discussion). For the oil phantom, the measured SNR for the fat-separated image using the multiecho Dixon PSIR late-enhancement protocol was 108.4 vs. 138.2 using the conventional PSIR late-enhancement protocol.

The SNR of the multiecho Dixon fat-separated image using the precontrast protocol was 192 (oil phantom), compared with 396 (oil phantom) for the corresponding conventional TSE image. The multiecho Dixon fat-sepa-
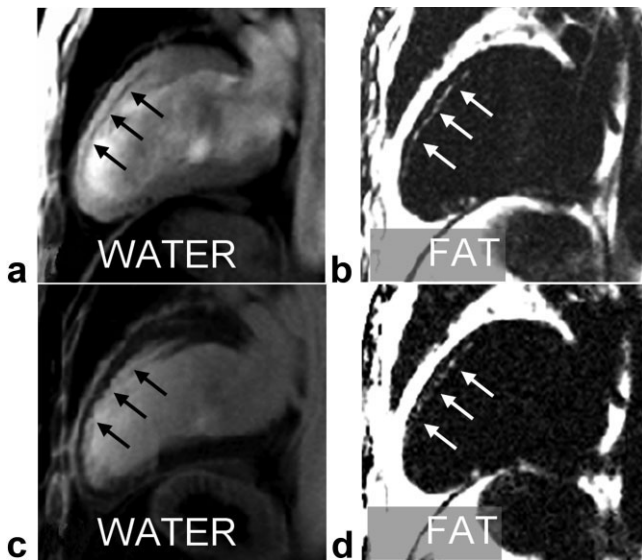
FIG. 2. Water- and fat-separated images using the multiecho Dixon method for a patient with chronic MI showing fatty infiltration: (**a** and **b**) precontrast and (**c** and **d**) PSIR late enhancement.
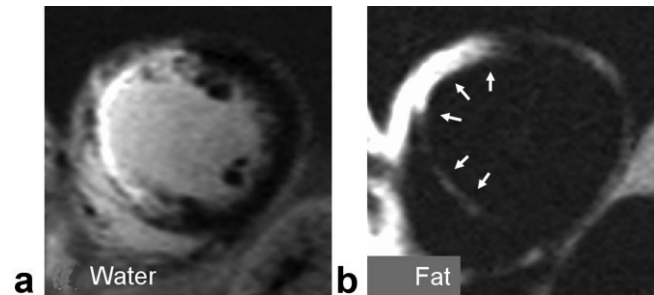

FIG. 3. PSIR water- and fat-separated late-enhancement images acquired in a single breath-hold using the multiecho Dixon method for a patient with chronic MI showing fibrofatty infiltration: (**a**) water and (**b**) fat.

rated image had approximately half the SNR of the TSE image (without parallel imaging).

The SNR of the multiecho Dixon fat-separated image was compared between the precontrast protocol (192) and the late-enhancement protocol (108.3). The precontrast protocol yielded approximately 1.8 times the SNR as the late-enhancement protocol, which uses IR.

Patient Images

The technique was applied successfully in all 28 patients. Of the 10 studies with indication of CAD, there were 8 cases with MI (one acute and seven chronic), of which four cases with chronic MI exhibited fatty infiltration. Water- and fat-separated images for a case with fatty infiltration in chronic anteroseptal MI are shown in Fig. 2 for both precontrast (a and b) and PSIR late enhancement (c and d). The phase-encode (PE) direction is horizontal in all of the figures. The measured SNR of the fatty infiltration was 4.0 ± 1.4 (m $\pm$ SD, $N = 4$) measured by PSIR late enhancement. There were five chronic MI cases in which both pre- and postcontrast water- and fat-separated images were acquired. The SNR of epicardial fat was measured since only two of these five cases had fatty infiltration in the MI. The measured SNR of the epicardial fat signal was 71.7 ± 29.5 precontrast vs. 27.6 ± 11.1 postcontrast, $N = 5$ cases (m $\pm$ SD). Water- and fat-separated PSIR late-enhancement images (Fig. 3) are shown for one additional patient with chronic MI with fatty infiltration. The overall infarct image quality is quite good and comparable to conventional late enhancement without water and fat separation, with the water-separated image yielding the same diagnostic quality as the conventional late-enhancement image in all of the cases, despite a slight reduction in SNR.

A total of 13 studies were conducted to rule out ARVC in patients typically referred due to family history or arrhythmias. There were four cases of atypical late enhancement,

of which three cases had intramyocardial fatty infiltration (one case confirmed by biopsy of the septum). In one case (Fig. 4) the patient was diagnosed with myocardial lipodystrophy because the case did not meet Task Force criteria for the diagnosis of ARVC. A second case (Fig. 5) with fibrofatty infiltration (confirmed by needle biopsy) met the diagnostic Task Force criteria for ARVC (more than two major criteria of different categories). A third case was confirmed to have ARVC, meeting one major and two minor Task Force criteria. A fourth ARVC rule-out study met only a single major criterion for ARVC. Intramyocardial fat was present in the apical septal region; however, apical fat is a frequent finding in normal hearts (1). The remaining nine cases did not meet the criteria for ARVC.

In these ARVC rule-out studies of cases with fibrofatty infiltration, the multiecho Dixon water- and fat-separated images acquired in a single breath-hold were compared
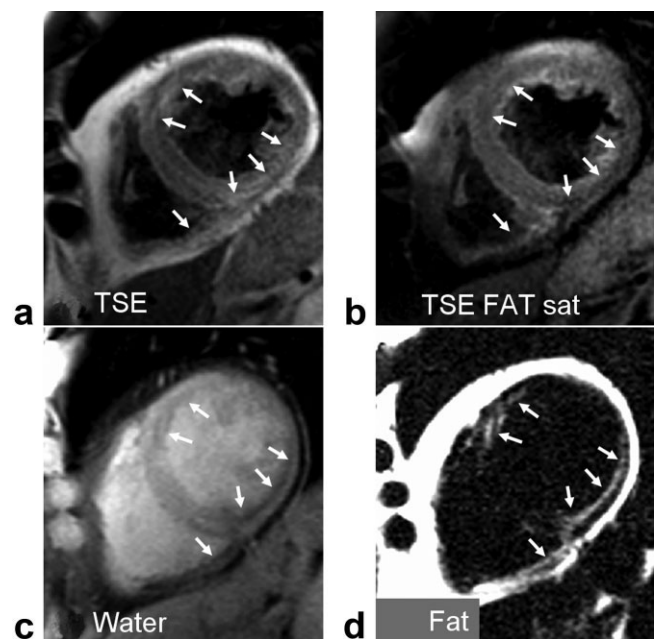

FIG. 4. Patient with myocardial lipodystrophy. Intramyocardial fat is clearly evident in the fat-separated image using the multiecho Dixon method (**d**), which is difficult to discern in the conventional fat-suppressed image (**b**).
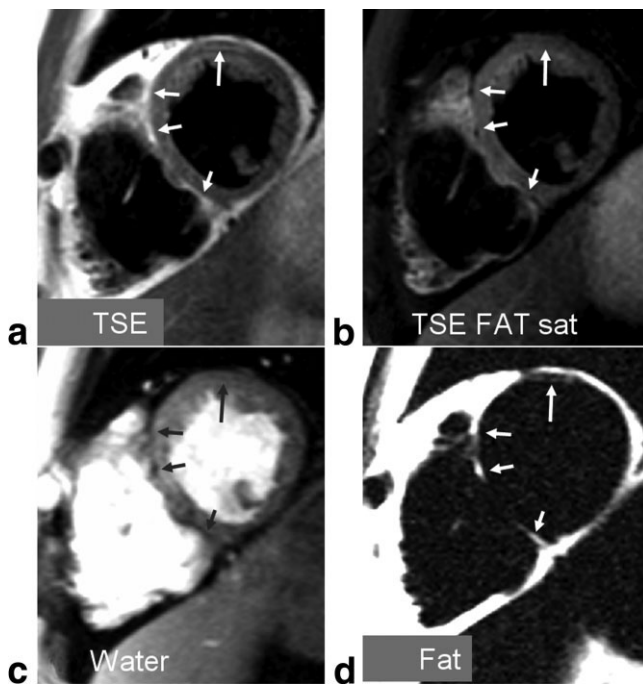
FIG. 5. Patient with ARVC showing intramyocardial fat clearly evident in the fat-separated image (**d**), which is difficult to discern in the conventional fat-suppressed image (**b**).

with the conventional approach using dark-blood-prepared TSE acquired with and without chemical-shift fat saturation in two separate breath-holds. In the first patient with fibrofatty infiltration (Fig. 4) intramyocardial fat is clearly evident in the fat-separated image (Fig. 4d) but difficult to discern in the conventional fat-suppressed dark-blood TSE image (Fig. 4b). Fat is observed (see arrows) in endocardial regions of both LV and RV myocardium. In the second patient with confirmed ARVC (Fig. 5), intramyocardial fat is evident in the septum and anterior sector (longer arrow) of LV myocardium. This is more readily discerned in the fat-separated image (Fig. 5d), which has positive contrast, than by comparison of TSE images acquired with and without chemical-shift fat suppression (Fig. 5a and b).

In the above three cases in which fibrofatty infiltration was detected using the proposed multiecho Dixon water- and fat-separation method, the measured CNR of the fat signal was 14.0 ± 3.8 (mean $\pm$ SD, $N = 3$). In these same cases fatty infiltration could be detected in two of the three cases using the conventional TSE with and without chemical-shift fat suppression, and the measured CNR was 5.8 ± 3.1 ($N = 2$). Thus, the CNR of the multiecho Dixon method was 2.4 times higher than conventional TSE in these cases. The TSE images for the third case were acquired at a different slice orientation where fat was not detected.

Five patients had been referred for suspected cardiac masses. One patient had a large lipoma (Fig. 6) and another had a region with lipomatous hypertrophy of the interatrial septum. While fat suppression of the epicardial fat and the lipoma mass (Fig. 6b) was excellent, the water- and fat-separated images (Fig. 6c and d) had even greater contrast.

Epicardial fat was readily distinguished from myocardium in all cases of water- and fat-separated images.

DISCUSSION

The proposed approach can characterize intramyocardial fat before or after contrast administration. A benefit of using late enhancement with fat-water separation is the ability to display contrast-enhanced myocardial fibrosis in the water image and fatty infiltration in the fat image, with both acquired simultaneously. Initial experience indicates a much higher contrast and sensitivity than conventional fat suppression. The fat-separated image has positive contrast against a noise background, providing greater confidence in detection than conventional fat suppression, which is often difficult to discriminate from fluctuations in the water signal. Consider the example of chronic MI shown in Fig. 3. In the septal region, the SNR of the MI water signal is approximately 38, and fat in this same region has an SNR of 5.3 corresponding to a water/fat signal ratio of 7.2 (i.e., <15% fat). The fat signal in the fat-separated image is readily detectable against the noise background; however, if the myocardial signal fluctuation for a conventional fat-suppressed image due to stagnant blood signal, Gibb's ringing, or other effects was on the order of 10–20%, the detectability of the hypointense signal region due to fat would be greatly reduced. In the cases of Figs. 4b and 5b, it would be difficult to make a diagnosis of intramyocardial fat with high confidence despite reasonably good fat saturation.

The dark-blood preparation commonly used with TSE imaging often leads to bright stagnant blood artifacts in the trabeculae and along the endocardial border, as well as posterior wall signal loss due to cardiac motion, which further complicates the image interpretation (Fig. 4).
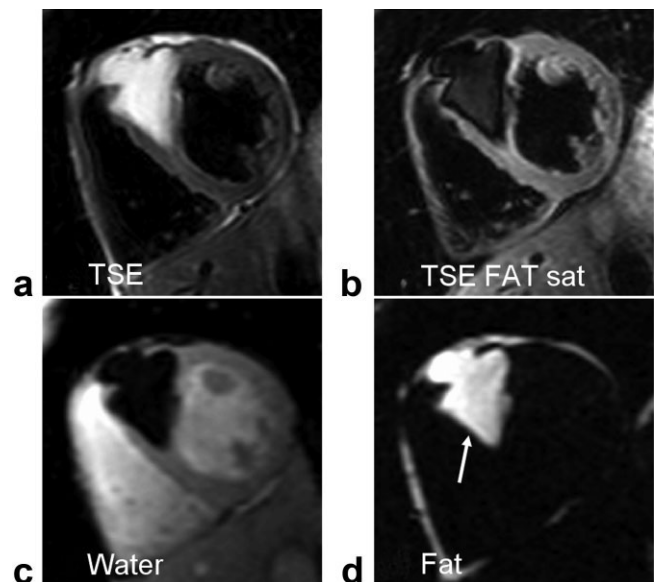

FIG. 6. Precontrast images for a patient with a large anteroseptal lipoma: (**a**) TSE without fat saturation and (**b**) TSE with fat saturation, acquired in two separate breathholds; and (**c**) water- and (**d**) fat-separated images acquired in a single breathhold using a multiecho Dixon approach.

Therefore, although dark-blood-prepared TSE has the potential to achieve a high SNR, the loss in CNR due to signal inhomogeneity makes this approach less reliable in clinical practice. The measured CNR of the myocardial infiltrated fat signal was 2.4 times better for the multiecho fat-separated image than for dark-blood TSE with chemical-shift fat suppression. Furthermore, conventional fat suppression is highly dependent on the ability to shim the inhomogeneous background field.

Phase-sensitive reconstruction is insensitive to TI, which is particularly important when assessing atypical late enhancement with a patchy appearance. The proposed method has the additional benefit of using a single breath-hold to produce fat and water images, thereby improving the workflow and ensuring spatial registration. The VARPRO method provided robust fieldmap estimates.

The use of multiecho Dixon fat-water separation with three echoes at nonoptimum TEs may be ill-conditioned and not achieve the full SNR gain (effective NSA). Although optimum TEs calculated for the case of three echoes (16) were not achievable using monopolar readout, the four-echo implementation is very robust and achieved within 5% of the optimum expected SNR (four effective averages) almost completely independently of the water/fat ratio (Fig. 1). Conventional late enhancement using a segmented turboFLASH sequence without water and fat separation uses a lower bandwidth with slightly shorter TR (e.g., 140 Hz/pixel and 8 ms). Using the parameters of this study, the SNR loss for the four-echo water- and fat-separated approach compared to the conventional method is approximately $\sqrt{977/(140 \times 4)}$ = 1.32 or 32%. The actual SNR loss is slightly less due to the longer TR. The SNR loss may be reduced by using a lower bandwidth. Using the Siemens 1.5T MAGNETOM Avanto (45 mT/m, SR = 200 T/m/s), the same TEs and TR may be achieved using a bandwidth of 723 Hz/pixel. With this bandwidth, the SNR loss may be reduced to approximately 14%.

The SNR of precontrast, multiecho, fat-separated images was approximately 2.6 times that of postcontrast late enhancement using IR with the given protocol. The late-enhancement fat signal depends on the TI. Despite the SNR loss, the added benefit of postcontrast late-enhancement imaging is that a positive correlation of fat with fibrous tissue can be attained in spatially registered images acquired simultaneously. The improved SNR of the precontrast images provides additional confidence in situations where both protocols may be acquired.

A benefit of the multiecho Dixon method is the mitigation of the chemical-shift artifact (9,10). Conventional late-enhancement imaging using 140 Hz/pixel has a significant chemical-shift artifact where the fat is displaced relative to the water in the readout direction by approximately 1.5 pixels. The multiecho Dixon approach, which uses a much larger bandwidth, has a subpixel shift (0.2 pixel) and, if necessary, may be completely eliminated as described above in Materials and Methods. Using the conventional approach, the epicardial fat may be displaced by as much as 30% of the diastolic wall thickness.

The presence of intramyocardial fat in diseases such as ARVC may form a substrate for reentrant ventricular arrhythmias leading to sudden death (1,17–20). Analysis of autopsies has shown that fibrofatty infiltration into the myocardium was more predictive of sudden death than simple fatty infiltration (1). However, due to the subjectivity of interpreting the presence of intramyocardial fat using conventional fat-suppression methods, MRI fibrofatty infiltration is not part of the currently accepted Task Force criteria (17). The proposed multiecho Dixon method may be helpful in the diagnosis of patients with ARVC due to the improved fat-myocardial contrast. The prognostic significance of fibrofatty infiltration in chronic MI is currently unknown, but is potentially of interest in predicting arrhythmias or prognosis. Pericardial fat accumulation may also be used as a predictor of CAD (21). The fat-separated images may be useful for quantifying the amount of pericardial fat.

CONCLUSIONS

The multiecho Dixon method for fat and water separation provides a sensitive means of detecting intramyocardial fat with positive signal contrast, thereby achieving a high degree of confidence, whereas conventional fat suppression is often difficult to interpret due to fluctuations in the water signal. The proposed water- and fat-separation method is combined simultaneously with late-enhancement imaging to provide a positive correlation between fibrosis and fat. The proposed VARPRO approach to multiecho Dixon water and fat separation is robust for clinical application to cardiac imaging. Using the proposed method, fibrofatty infiltration has been observed in chronic MI as well as cases with ARVC. This technique could be used to assess the prognostic value of the presence and amount of myocardial fat infiltration.

ACKNOWLEDGMENTS

REFERENCES

1. Burke AP, Farb A, Tashko G, Virmani R. Arrhythmogenic right ventricular cardiomyopathy and fatty replacement of the right ventricular myocardium: are they different diseases? Circulation 199828;97:1571–1580.
2. Dixon W. Simple proton spectroscopic imaging. Radiology 1984;153: 189–194.
3. Glover GH, Schneider E. Three-point Dixon technique for true water/fat decomposition with B0 inhomogeneity correction. Magn Reson Med 1991;18:371–383.
4. Szumowski J, Coshow WR, Li F, Quinn SF. Phase unwrapping in the three-point Dixon method for fat suppression MR imaging. Radiology 1994;192:555–561.
5. Reeder SB, Wen Z, Yu H, Pineda AR, Gold GE, Markl M, Pelc NJ. Multicoil Dixon chemical species separation with an iterative least-squares estimation method. Magn Reson Med 2004;51:35–45.
6. Reeder SB, Pineda AR, Wen Z, Shimakawa A, Yu H, Brittain JH, Gold GE, Beaulieu CH, Pelc NJ. Iterative decomposition of water and fat with echo asymmetry and least-squares estimation (IDEAL): application with fast-spin echo imaging. Magn Reson Med 2005;54:636–644.
7. Yu H, Reeder SB, Shimakawa A, Brittain JH, Pelc NJ. Field map estimation with a region growing scheme for iterative 3-point water-fat decomposition. Magn Reson Med 2005;54:1032–1039.
8. Hernando D, Haldar JP, Sutton BP, Ma J, Kellman P, Liang Z-P. Joint estimation of water/fat images and field inhomogeneity map. Magn Reson Med 2008;59:571-580.

9. Haacke EM, Brown RW, Thompson MR, Venkatesan R. Magnetic resonance imaging: physical principles and sequence design. New York: John Wiley & Sons; 1999. p 421–449.

10. Stark DD, Bradley Jr WG. Magnetic resonance imaging. St. Louis: Mosby Inc. p 159–179.

11. Golfarb JW, Arnold S, Roth M, Han J. T1-weighted magnetic resonance imaging shows fatty deposition after myocardial infarction. Magn Reson Med 2007;57:828–834.

12. Reeder SB, Faranesh AZ, Boxerman JL, McVeigh ER. In vivo measurement of T2* and field inhomogeneity maps in the human heart at 1.5 T. Magn Reson Med 1998;39:988–998.

13. Kellman P, Arai AE, McVeigh ER, Aletras AH. Phase sensitive inversion recovery for detecting myocardial infarction using gadolinium delayed hyperenhancement. Magn Reson Med 2002;47:372–383.

14. Lu W, Reeder SB, Daniel BL, Hargreaves BA. Chemical shift correction in bipolar multi-echo sequences for water and fat separation. In: Proceedings of the 15th Annual Meeting of ISMRM, Berlin, Germany, 2007 (Abstract 1622).

15. Kellman P, McVeigh ER. Image reconstruction in SNR units: a general method for SNR measurement. [Published erratum in Magn Reson Med 2007;58:211–212]. Magn Reson Med 2005;54:1439–1447.

16. Pineda AR, Reeder SB, Wen Z, Pelc NJ. Cramer-Rao bounds for three-point decomposition of water and fat. Magn Reson Med 2005;54:625–635.

17. Bluemke DA, Krupinski EA, Ovitt T, Gear K, Unger E, Axel L, Boxt LM, Casolo G, Ferrari VA, Funaki B, Globits S, Higgins CB, Julsrud P, Lipton M, Mawson J, Nygren A, Pennell DJ, Stillman A, White RD, Wichter T, Marcus F. MR imaging of arrhythmogenic right ventricular cardiomyopathy: morphologic findings and interobserver reliability. Cardiology 2003;99:153–162.

18. Tandri H, Castillo E, Ferrari VA, Nasir K, Dalal D, Bomma C, Calkins H, Bluemke DA. Magnetic resonance imaging of arrhythmogenic right ventricular dysplasia: sensitivity, specificity, and observer variability of fat detection versus functional analysis of the right ventricle. J Am Coll Cardiol 20065;48:2277–2284.

19. Tandri H, Saranathan M, Rodriguez ER, Martinez C, Bomma C, Nasir K, Rosen B, Lima JA, Calkins H, Bluemke DA. Noninvasive detection of myocardial fibrosis in arrhythmogenic right ventricular cardiomyopathy using delayed-enhancement magnetic resonance imaging. J Am Coll Cardiol 2005;45:98–103.

20. Sen-Chowdhry S, Prasad SK, Syrris P, Wage R, Ward D, Merrifield R, Smith GC, Firmin DN, Pennell DJ, McKenna WJ. Cardiovascular magnetic resonance in arrhythmogenic right ventricular cardiomyopathy revisited: comparison with task force criteria and genotype. J Am Coll Cardiol 2006;48:2132–2140.

21. Taguchi R, Takasu J, Itani Y, Yamamoto R, Yokoyama K, Watanabe S, Masuda Y. Pericardial fat accumulation in men as a risk factor for coronary artery disease. Atherosclerosis 2001;157:203–209.